Proceedings of the 16th International Conference on Computational and Mathematical Methods in Science and Engineering, CMMSE 2016 4–8 July, 2016.

# Quantum Wigner molecules in semiconductor quantum dots and cold-atom optical traps and their mathematical symmetries

#### Constantine Yannouleas<sup>1</sup> and Uzi Landman<sup>1</sup>

<sup>1</sup> School of Physics, Georgia Institute of Technology, Atlanta, GA 30332-0430, USA emails: Constantine.Yannouleas@physics.gateh.edu,
Uzi.Landman@physics.gateh.edu

#### Abstract

Strong repelling interactions between a few fermions or bosons confined in twodimensional circular traps lead to particle localization and formation of quantum Wigner molecules (QWMs) possessing definite point-group space symmetries. These pointgroup symmetries are "hidden" (or emergent), namely they cannot be traced in the circular single-particle densities (SPDs) associated with the exact many-body wave functions, but they are manifested as characteristic signatures in the ro-vibrational spectra. An example, among many, are the few-body QWM states under a high magnetic field or at fast rotation, which are precursor states for the fractional quantum Hall effect. The hidden geometric symmetries can be directly revealed by using spin-resolved conditional probability distributions, which are extracted from configuration-interaction (CI), exact-diagonalization wave functions. The hidden symmetries can also be revealed in the CI SPDs by reducing the symmetry of the trap (from circular to elliptic to quasi-linear). In addition the hidden symmetries are directly connected to the explicitly broken-symmetry (BS) solutions of mean-field approaches, such as unrestricted Hartree-Fock (UHF). A companion step of restoration of the broken symmetries via projection operators applied on the BS-UHF solutions produces wave functions directly comparable to the CI ones, and sheds further light into the role played by the emergence of hidden symmetries in the exact many-body wave functions. Illustrative examples of the importance of hidden symmetries in the many-body problem of few electrons in semiconductor quantum dots and of few ultracold atoms in optical traps (where unprecedented control of the interparticle interaction has been experimentally achieved recently) will be presented.

Key words: Wigner molecule, emergent point-group symmetries, broken symmetries, symmetry restoration, projection operator, unrestricted Hartree Fock, configuration interaction, 2D semicoductor quantum dots, trapped ultracold atoms, fermions, bosons

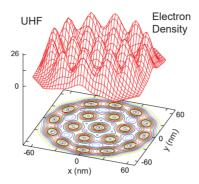


Figure 1: Unrestricted Hartree-Fock electron density in a 2D parabolic QD for N=19 electrons and total-spin projection  $S_z=19/2$ , exhibiting breaking of the circular symmetry at  $R_W=5$  and zero magnetic field. The electrons are (partially) localized in a (1,6,12) multi-ring structure, which exhibits point-group symmetries. Remaining parameters are: parabolic confinement,  $\hbar\omega_0=5$  meV; effective mass  $m^*=0.067m_e$ . Distances are in nanometers and the electron density in  $10^{-4}$  nm<sup>-2</sup>.

### 1 Introduction

This talk focuses on novel, somewhat exotic, types of clusters of few fermions or bosons. In particular, we discuss clusters of electrons in manmade (artificial) quantum dots (QDs) created through lithographic and gate-voltage techniques at semiconductor interfaces, and clusters of neutral ultracold atoms (either bosonic or fermionic) in harmonic optical traps. These cluster systems exhibit interesting emergent physical behavior arising from spontaneous breaking of spatial and/or spin symmetries at the mean-field level of theoretical treatment [1, 2]; symmetry breaking (SB) is defined as a circumstance where a lower energy solution of the Schrödinger equation is found that is characterized by a lower symmetry than that of the full many-body Hamiltonian of the few-body system. Such SB in circular traps directly reflects the localization of of particles in cluster arrangements exhibiting point-group symmetries instead of the continuous rotational symmetry expected from the many-body Hamiltonian [2]. A prominent example is the formation of finite electron crystallites (referred to as semi-classical Wigner molecules, SCWMs) in two-dimensional (2D) QDs (see Fig. 1). Symmetry breaking at the mean-field level is also manifested in the transition [3, 4], induced by increasing the interatomic repulsive contact-interaction strength, of the ground state of neutral atoms in a parabolic or toroidal 2D trap to a rotating bosonic quantum Wigner molecule (QWM). An example is presented in Fig. 2, where the hierarchy of the successive approximations (broken symmetry UHF  $\rightarrow$  symmetry restoration) is illustrated, leading to the symmetry-restored, fully-quantal wave function (QWM) in Fig. 2 (c,d); the single-particle density (SPD) for the intermediate BS-UHF (SCWM) wave func-

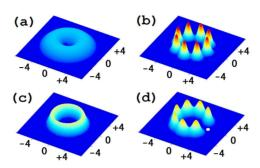


Figure 2: Single-particle densities and CPDs for N=8 neutral repelling bosons in a rotating 2D toroidal trap with reduced rotational frequency  $\Omega/\omega_0=0.2$  and  $R_\delta=50$ . The confining potential,  $m\omega_0^2(r-r_0)^2/2$ , is centered at a radius  $r_0=3l_0$ . (a) Gross-Pitaevski SPD. (b) UHF SPD exhibiting breaking of the circular symmetry. (c) QWM SPD exhibiting circular symmetry. (d) CPD for the QWM wave function (resulting from the method of symmetry restoration), revealing the hidden point-group symmetry in the intrinsic frame of reference. The fixed observation point is denoted by a white dot. The QWM ground-state angular momentum is  $L_z=16$ . Lengths in units of the oscillator length  $l_0$ . The vertical scale is the same for (b), (c), and (d), but different for (a).

tion is plotted in Fig. 2(b). Note that the point-group symmetry is not visible in the SPD after the step of symmetry restoration is executed, i.e., it becomes hidden [see Fig. 2(c)], but it is revealed via a conditional probability distribution (CPD); see Fig. 2(d).

The CPD gives the probability of finding a particle with spin  $\sigma$  at position  $\mathbf{r}$  given that another one (referred to as the fixed particle) with spin  $\sigma_0$  is located at  $\mathbf{r}_0$ . The degree of particle localization is controlled by the Wigner parameter that specifies the strength of the interparticle repulsion relative to the zero-point kinetic energy, i.e.,  $R_W = Z^2 e^2/(\kappa l_0 \hbar \omega_0)$  [2, 3] for a Coulomb repulsion and  $R_{\delta} = gm/(2\pi\hbar^2)$  [2, 3, 4] for a contact-potential (Diracdelta) repulsion; Z is the charge of the particle,  $\kappa$  is the dielectric constant,  $\omega_0$  is the frequency of the harmonic trap,  $l_0 = \sqrt{\hbar/(m\omega_0)}$  is the oscillator length, m is the particle mass, and q is the strength of the contact interaction.

Of great value in analyzing the physics associated with the hidden symmetries is the evolution of the lowest-energy band in the energy spectra (yrast band) as a function of the two successive approximations (broken symmetry UHF  $\rightarrow$  symmetry restoration). Figs. 3(a,b) present the evolution of yrast spectra (as a function of the rotational frequency  $\Omega$  of the trap) that are associated with the class of wave functions portrayed in Fig. 2. The most prominent trend is that the ground-state angular momenta of the symmetry-restored wave functions do not assume all the possible 2D values, but are restricted to stepwise values  $L_z = Nk, k = 0, 1, 2, \ldots$ , with N = 8, i.e., they change in steps of N = 8, where N is

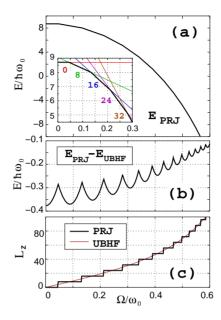


Figure 3: Properties of N=8 neutral repelling bosons in a rotating 2D toroidal trap as a function of the reduced rotational frequency  $\Omega/\omega_0$ . The confining toroidal potential is centered at a radius  $r_0=3l_0$ , and the interaction-strength parameter was chosen as  $R_\delta=50$ . (a) QWM ground-state energies,  $E^{PRJ}$ . The term QWM corresponds to projected (PRJ) wave functions that preserve the total angular momentum (symmetry restoration). The inset shows the range  $0 \le \Omega/\omega_0 \le 0.3$ . The numbers denote ground-state magic angular momenta. (b) Energy difference  $E^{PRJ} - E^{UBHF}$ , where the subscript "UBHF" stands for unrestricted bosonic Hartree-Fock. (c) Total angular momenta associated with (i) the QWM ground states [thick solid line (showing steps and marked as PRJ); online black] and (ii) the broken-symmetry UBHF solutions (smooth thin solid line; online red).

the number of particles [see Fig. 3(c) and the inset in Fig. 3(a)]. Such stepwise angular momenta are usually referred to as "magic" and the associated ground states of enhanced stability [see Fig. 3(b)] are finite-size precursors of the bulk fractional quantum Hall states; see also Section 3 below.

# 2 Group theoretical analysis of symmetry breaking in unrestricted Hartree Fock

We mention here the case of N=3 fully spin polarized  $(S_z=3/2)$  electrons in the absence of a magnetic field (B) and for  $R_W=10$  ( $\kappa=1.9095$ ). Fully spin polarized UHF determinants

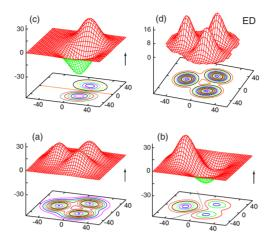


Figure 4: The UHF case exhibiting breaking of the circular symmetry for N=3 electrons and total spin projection  $S_z=3/2$  at  $R_W=10$  and at zero magnetic field. (a-c): real orbitals (modulus square). (d): the corresponding electron density (ED). The choice of the remaining parameters is:  $\hbar\omega_0=5$  meV and effective mass  $m^*=0.067m_e$ . Distances are in nanometers. The real orbitals are in  $10^{-3}$  nm<sup>-1</sup> and the total ED in  $10^{-4}$  nm<sup>-2</sup>. The arrows indicate the spin projection  $(S_z=1/2)$  for each orbital.

preserve the total spin, but for this value of  $R_W$  the lowest in energy UHF solution is one with broken circular symmetry. As it has been mentioned earlier, broken rotational symmetry does not imply no space symmetry, but a lower point-group symmetry [5].

In Fig. 4 we display the UHF symmetry-violating orbitals (a-c) whose energies are (a) 44.801 meV, (b) and (c) 46.546 meV, namely the two orbitals (b) and (c) with the higher energies are degenerate in energy. Overall the BS orbitals (a-c) drastically differ from the orbitals of the independent particle model. In particular, they are associated with specific sites (within the QD) forming an equilateral triangle, and thus they can be described as having the structure of a linear combination of "atomic" (site) orbitals (LCAOs). Such LCAO molecular orbitals (MOs) are familiar in natural molecules, and this analogy supports the term "semi-classical electron (or Wigner) molecules" for characterizing the BS-UHF solutions. We notice here that the LCAO orbitals in Fig. 4 are familiar in Organic Chemistry and are associated with the theoretical description of Carbocyclic Systems, and in particular the molecule C<sub>3</sub>H<sub>3</sub> (cyclopropenyl, see, e.g., Ref. [6]). The important point of course is not the uniqueness or not of the 2D UHF orbitals, but the fact that they transform according to the irreducible representations of specific point groups, leaving both the UHF determinant and the associated electron densities invariant.

The electron density (ED) portrayed in Fig. 4(d) remains invariant under certain geo-

Table 1: Character table for the cyclic group  $C_3$  [ $\varepsilon = \exp(2\pi i/3)$ ]

$$\begin{array}{c|ccccc} & C_3 & E & C_3 & C_3^2 \\ \hline A & 1 & 1 & 1 \\ E' & 1 & \varepsilon & \varepsilon^* \\ E'' & 1 & \varepsilon^* & \varepsilon \end{array}$$

metrical symmetry operations, namely those of an unmarked, plane and equilateral triangle. They are: (1) The identity E; (2) The two rotations  $C_3$  (rotation by  $2\pi/3$ ) and  $C_3^2$  (rotation by  $4\pi/3$ ); and (III) The three reflections  $\sigma_v^I$ ,  $\sigma_v^{II}$ , and  $\sigma_v^{III}$  through the three vertical planes, one passing through each vertex of the triangle. These symmetry operations for the unmarked equilateral triangle constitute the elements of the group  $C_{3v}$  [6, 7].

One of the main applications of group theory in Chemistry is the determination of the eigenfunctions of the Schrödinger equation by simply using symmetry arguments alone. This is achieved by constructing the so-called *symmetry-adapted linear combinations* (SALCs) of AOs. A widely used tool for constructing SALCs is the projection operator

$$\hat{\mathcal{P}}^{\mu} = \frac{n_{\mu}}{|\mathcal{G}|} \sum_{R} \chi^{\mu}(R) \hat{R}, \tag{1}$$

where  $\hat{R}$  stands for any one of the symmetry operations of the molecule, and  $\chi^{\mu}(R)$  are the characters of the  $\mu$ th irreducible representation of the set of  $\hat{R}$ 's. (The  $\chi^{\mu}$ 's are tabulated in the socalled character tables [6, 7].)  $|\mathcal{G}|$  denotes the order of the group and  $n_{\mu}$  the dimension of the representation.

The task of finding the SALCs for a set of three 1s-type AOs exhibiting the  $C_{3v}$  symmetry of an equilateral triangle can be simplified, since the pure rotational symmetry by itself (the rotations  $C_3$  and  $C_3^2$ , and not the reflections  $\sigma_v$ 's through the vertical planes) is sufficient for their determination. Thus one needs to consider the simpler character table of the cyclic group  $C_3$  (see Table 1).

From Table 1, one sees that the set of the three 1s AOs situated at the vertices of an equilateral triangle spans the two irreducible representations A and E, the latter one consisting of two associted one-dimensional representations. To construct the SALCs, one simply applies the three projection operators  $\hat{\mathcal{P}}^A$ ,  $\hat{\mathcal{P}}^{E'}$ , and  $\hat{\mathcal{P}}^{E''}$  to one of the original AOs, let's say the  $\phi_1$ ,

$$\hat{\mathcal{P}}^{A}\phi_{1} \approx (1)\hat{E}\phi_{1} + (1)\hat{C}_{3}\phi_{1} + (1)\hat{C}_{3}^{2}\phi_{1} = (1)\phi_{1} + (1)\phi_{2} + (1)\phi_{3}$$

$$= \phi_{1} + \phi_{2} + \phi_{3}, \tag{2}$$

$$\hat{\mathcal{P}}^{E'}\phi_1 \approx (1)\hat{E}\phi_1 + (\varepsilon)\hat{C}_3\phi_1 + (\varepsilon^*)\hat{C}_3^2\phi_1 = \phi_1 + \varepsilon\phi_2 + \varepsilon^*\phi_3,\tag{3}$$

$$\hat{\mathcal{P}}^{E''}\phi_1 \approx (1)\hat{E}\phi_1 + (\varepsilon^*)\hat{C}_3\phi_1 + (\varepsilon)\hat{C}_3^2\phi_1 = \phi_1 + \varepsilon^*\phi_2 + \varepsilon\phi_3. \tag{4}$$

The A SALC in Eq. (2) is real. The two E SALCs [Eq. (3) and Eq. (4)], however, are complex functions and do not coincide with the real UHF orbitals. These complex SALCs agree with BS-UHF orbitals obtained in the case of an applied magnetic field. On the other hand, a set of two real and orthogonal SALCs that spans the E representation can be derived fron Eq. (3) and Eq. (4) by simply adding and substracting the two complex ones. This procedure recovers immediately the real UHF orbitals displayed in Fig. 4.

# 3 Restoration of circular symmetry: Group structure and sequences of magic angular momenta

In the previous section, we discussed how the BS-UHF determinants and orbitals describe indeed 2D molecular stuctures (semi-classical Wigner molecules) in close analogy with the case of natural 3D molecules. However, the study of the WMs at the UHF level restricts their description to the *intrinsic* (nonrotating) frame of reference. Motivated by the case of natural atoms, one can take a subsequent step and address the properties of *collectively* rotating QWMs in the laboratory frame of reference. As is well known, for natural atoms, this step is achieved by writing the total wave function of the molecule as the product of the electronic and ionic partial wave functions. In the case of the purely electronic or bosonic WMs, however, such a product wave function requires the assumption of complete decoupling between intrinsic and collective degrees of freedom, an assumption that might be justifiable in limiting cases only.

Using the BS UHF solutions, this subsequent step can be addressed by using the post-Hartree-Fock method of restoration of broken symmetries [2, 8] via projection (PRJ) techniques.

In this section, we will use the PRJ approach to illustrate how certain universal properties of the CI (exact) solutions, i.e., the appearance of magic angular momenta in the exact rotational spectra, [2, 9, 10, 11, 12, 13] relate to the symmetry broken UHF solutions. Indeed, we will demonstrate that the magic angular momenta are a direct consequence of the symmetry breaking at the UHF level and that they are determined fully by the molecular symmetries of the UHF determinant.

As an illustrative example, we have chosen the relatively simple, but non trivial case, of N=3 electrons. For B=0, both the  $S_z=1/2$  and  $S_z=3/2$  polarizations can be considered. We start with the  $S_z=1/2$  polarization, whose BS UHF solution (let's denote it by  $|\downarrow\uparrow\uparrow\rangle$ ) exhibits a breaking of the total spin symmetry in addition to the rotational symmetry. We first proceed with the restoration of the total spin by noticing that  $|\downarrow\uparrow\uparrow\rangle$  has a point-group symmetry lower than the  $C_{3v}$  symmetry of an equilateral triangle. The  $C_{3v}$  symmetry, however, can be readily restored by applying the projection operator in Eq. (1) to  $|\downarrow\uparrow\uparrow\rangle$  and by using the character table of the cyclic  $C_3$  group (see Table 1). Then for the

intrinsic part of the many-body wave function, one finds two different three-determinantal combinations, namely

$$\Phi_{intr}^{E'}(\gamma_0) = |\downarrow\uparrow\uparrow\rangle + e^{2\pi i/3}|\uparrow\downarrow\uparrow\rangle + e^{-2\pi i/3}|\uparrow\uparrow\downarrow\rangle, \tag{5}$$

and

$$\Phi_{intr}^{E''}(\gamma_0) = |\downarrow\uparrow\uparrow\rangle + e^{-2\pi i/3}|\uparrow\downarrow\uparrow\rangle + e^{2\pi i/3}|\uparrow\uparrow\downarrow\rangle, \tag{6}$$

where  $\gamma_0 = 0$  denotes the azimuthal angle of the vertex associated with the original spindown orbital in  $|\downarrow\uparrow\uparrow\rangle$ . We note that the intrinsic wave functions  $\Phi_{intr}^{E'}$  and  $\Phi_{intr}^{E''}$  are eigenstates of the square of the total spin operator  $\hat{\mathbf{S}}^2$  ( $\hat{\mathbf{S}} = \sum_{i=1}^3 \hat{\mathbf{s}}_i$ ) with quantum number s(s+1) = 3/4, (s=1/2)). This can be verified directly by applying  $\hat{\mathbf{S}}^2$  to them.

To restore the circular symmetry in the case of a (0, N) ring arrangement, one applies the projection operator [2, 8, 14],

$$2\pi \mathcal{P}_I \equiv \int_0^{2\pi} d\gamma \exp[-i\gamma(\hat{L} - I)] , \qquad (7)$$

where  $\hat{L} = \sum_{j=1}^{N} \hat{l}_j$  is the operator for the total angular momentum. Notice that the operator  $\mathcal{P}_I$  is a direct generalization of the projection operator in Eq. (1) to the case of the continuous cyclic group  $C_{\infty}$  [the phases  $\exp(i\gamma I)$  are the characters of  $C_{\infty}$ ].

The projected wave function,  $\Psi_{PRJ}$ , (having both good total spin and angular momentum quantum numbers) is of the form,

$$2\pi\Psi_{PRJ} = \int_0^{2\pi} d\gamma \Phi_{intr}^E(\gamma) e^{i\gamma I}, \qquad (8)$$

where now the intrinsic wave function [given by Eq. (5) or Eq. (6)] has an arbitrary azimuthal orientation  $\gamma$ . We note that, unlike the phenomenological Eckardt-frame model [13] where only a single product term is involved, the PRJ wave function in Eq. (8) is an average over all azimuthal directions of an infinite set of product terms. These terms are formed by multiplying the UHF intrinsic part  $\Phi_{intr}^{E}(\gamma)$  with the external rotational wave function  $\exp(i\gamma I)$  (the latter is properly characterized as "external", since it is an eigenfunction of the total angular momentum  $\hat{L}$  and depends exclusively on the azimuthal coordinate  $\gamma$ ).

The operator  $R(2\pi/3) \equiv \exp(-i2\pi L/3)$  can be applied onto  $\Psi_{PRJ}$  in two different ways, namely either on the intrinsic part  $\Phi_{intr}^E$  or the external part  $\exp(i\gamma I)$ . Using Eq. (5) and the property  $\hat{R}(2\pi/3)\Phi_{intr}^{E'} = \exp(-2\pi i/3)\Phi_{intr}^{E'}$ , one finds,

$$\hat{R}(2\pi/3)\Psi_{PRJ} = \exp(-2\pi i/3)\Psi_{PRJ},$$
(9)

from the first alternative, and

$$\hat{R}(2\pi/3)\Psi_{PRJ} = \exp(-2\pi I i/3)\Psi_{PRJ},$$
 (10)

from the second alternative. Now if  $\Psi_{PRJ} \neq 0$ , the only way that Eqs. (9) and (10) can be simultaneously true is if the condition  $\exp[2\pi(I-1)i/3] = 1$  is fulfilled. This leads to a first sequence of magic angular momenta associated with total spin s = 1/2, i.e.,

$$I = 3k + 1, \ k = 0, \pm 1, \pm 2, \pm 3, \dots$$
 (11)

Using Eq. (6) for the intrinsic wave function, and following similar steps, one can derive a second sequence of magic angular momenta associated with good total spin s = 1/2, i.e.,

$$I = 3k - 1, \ k = 0, \pm 1, \pm 2, \pm 3, \dots$$
 (12)

In the fully polarized case, the UHF determinant is denoted as  $|\uparrow\uparrow\uparrow\rangle$ , and it is already an eigenstate of  $\hat{\mathbf{S}}^2$  with quantum number s=3/2. Thus only the rotational symmetry needs to be restored, that is, the intrinsic wave function is simply  $\Phi^A_{intr}(\gamma_0) = |\uparrow\uparrow\uparrow\rangle$ . Since  $\hat{R}(2\pi/3)\Phi^A_{intr} = \Phi^A_{intr}$ , the condition for the allowed angular momenta is  $\exp[-2\pi Ii/3] = 1$ , which yields the following magic angular momenta,

$$I = 3k, \ k = 0, \pm 1, \pm 2, \pm 3, \dots$$
 (13)

We note that in high magnetic fields only the fully polarized case is relevant and that only angular momenta with k > 0 enter in Eq. (13) (see Refs. [15, 16]). In this case, in the thermodynamic limit, the partial sequence with k = 2q + 1, q = 0, 1, 2, 3, ... is directly related to the odd filling factors  $\nu = 1/(2q + 1)$  of the fractional quantum Hall effect [via the relation  $\nu = N(N-1)/(2I)$ ]. This suggests that the observed hierarchy of fractional filling factors in the quantum Hall effect may be viewed as a signature originating from the point group symmetries of the intrinsic wave function  $\Phi_{intr}$ , and thus it is a manifestation of symmetry breaking at the UHF mean-field level.

# 4 Summary

The analysis presented above concerning the relation between hidden symmetries and emergent signatures (e.g., magic amgular momenta) in the spectra of symmetry-restored mean-field wave functions applies also in the case of configuration-interaction, exact many body wave functions; see the review in Ref. [2]. The CI method requires large-scale, parallel computations, but it has the advantage of providing benchmark results due to the achieved high quantitative accuracy. We refer to this combination of mean-field and CI analysis as computational microscopy [17].

Recently, we have incorporated in our CI computer codes the option of Dirac-delta contact interactions, in addition to the long-range Coulomb one. Thus we have been able to analyze the wave function anatomy of a few untracold fermionic (<sup>6</sup>Li) atoms in single

and double optical traps, where the formation of quantum Wigner molecules can be associated with the emergence of Heisenberg antiferromagnetic behavior [17, 18, 19] and the creation of highly entangled states; e.g., the celebrated Bell states for two  $^6$ Li atoms. (Such behavior was earlier predicted in the case of strongly repelling electrons in double quantum dots [18].) The unprecedented experimental control of the interparticle interaction (from zero to infinite strength) achieved in the case of a few trapped ultracold atoms is enabling investigations of fundamental physics (such as high  $T_c$  and 1D and 2D magnetism) from a bottom-up perspective. In addition, in analogy with the field of 2D semiconductor double and triple QDs, it promises technological applications in the area of quantum information and quantum computing. Our computational-microscopy approach can be used to investigate the universal behavior in the strongly correlated regime of both ultracold fermionic or bosonic trapped atoms and confined electrons.

## Acknowledgements

This work is supported by the Office of Basic Energy Sciences of the US Department of Energy (Grant No. FG05- 86ER45234).

#### References

- [1] C. Yannouleas and U. Landman, Spontaneous symmetry breaking in single and molecular quantum dots, Phys. Rev. Lett. 82 (1999) 5325-5328; (E) Phys. Rev. Lett. 85 (2000) 2220
- [2] C. Yannouleas and U. Landman, Symmetry breaking and quantum correlations in finite systems: Studies of quantum dots and ultracold Bose gases, and related nuclear and chemical methods, Rep. Prog. Phys. **70** (2007) 2067-2148
- [3] I. ROMANOVSKY, C. YANNOULEAS AND U. LANDMAN, Crystalline Boson phases in harmonic traps: Beyond the Gross-Pitaevskii mean field, Phys. Rev. Lett. 93 (2004) 230405
- [4] I. ROMANOVSKY, C. YANNOULEAS, L.O. BAKSMATY AND U. LANDMAN, *Bosonic molecules in rotating traps*, Phys. Rev. Lett. **97** (2006) 090401
- [5] C. Yannouleas and U. Landman, Group theoretical analysis of symmetry breaking in two-dimensional quantum dots, Phys. Rev. B 68 (2003) 035325
- [6] F.A. COTTON, Chemical Applications of Group Theory, Wiley, New York, 1990
- [7] A.B. Wolbarst, Symmetry and Quantum Systems, Van Nostrand Reinold, New York, 1977

- [8] P. Ring and P. Schuck, The Nuclear Many-body Problem, Springer-Verlag, New York, 1980
- [9] S.M. GIRVIN AND T. JACH, Interacting electrons in two-dimensional Landau levels: Results for small clusters, Phys. Rev. B 28 (1983) 4506-4509
- [10] P.A. Maksym and T. Chakraborty, Quantum dots in a magnetic-field: Role of electron-electron interactions, Phys. Rev. Lett. 65 (1990) 108-111
- [11] W.Y. Ruan, Y.Y. Liu, C.G. Bao and Z.Q. Zhang, Origin of magic angular momenta in few-electron quantum dots, Phys. Rev. B 51 (1995) 7942-7945
- [12] T. Seki, Y. Kuramoto and T. Nishino, Origin of magic angular momentum in a quantum dot under strong magnetic field, J. Phys. Soc. Jpn. 65 (1996) 3945-3951
- [13] P.A. Maksym, Eckardt frame theory of interacting electrons in quantum dots, Phys. Rev. B **53** (1996) 10871-10886
- [14] C. Yannouleas and U. Landman, Strongly correlated wave functions for artificial atoms and molecules, J. Phys.: Condens. Matter 14 (2002) L591-L598
- [15] C. Yannouleas and U. Landman, Trial wave functions with long-range coulomb correlations for two-dimensional N-electron systems in high magnetic fields, Phys. Rev. B 66 (2002) 115315
- [16] C. Yannouleas and U. Landman, Quantum dots in high-magnetic fields: Rotating-Wigner-molecule versus composite-fermion approach, Phys. Rev. B 68 (2003) 035326
- [17] B.B. BRANDT, C. YANNOULEAS AND U. LANDMAN, Double-well ultracold-fermions computational microscopy: Wave-function anatomy of attractive-pairing and Wignermolecule entanglement and natural orbitals, Nano Lett. 15 (2015) 7105
- [18] YING LI, C. YANNOULEAS AND U. LANDMAN, Artificial quantum-dot helium molecules: Electronic spectra, spin structures and Heisenberg clusters, Phys. Rev. B 80 (2009) 045326
- [19] S. Murmann, F. Deuretzbacher, G. Zürn, J. Bjerlin, S.M. Reimann, L. Santos, T. Lompe and S. Jochim, *Antiferromagnetic Heisenberg spin chain of a few cold atoms in a one-dimensional trap*, Phys. Rev. Lett. **115** (2015) 215301